Petroleum Science
https://doi.org/10.1007/s12182-020-00542-x

ORIGINAL ARTICLE

Investigation on the biodegradation levels of super heavy oils by parameter-striping method and refined Manco scale: a case study from the Chepaizi Uplift of Junggar Basin

Xiang-Chun Chang[1,2] · Bing-Bing Shi[1] · Zhong-Quan Liu[3] · Yue Wang[1] · You-De Xu[3]

Received: 30 April 2020 / Accepted: 2 November 2020

Abstract
The Carboniferous volcanic reservoir in the Chepaizi Uplift became an exploration hot target in recent years for its substantial amount of oils discovered. However, most of the Carboniferous heavy oils were biodegraded to PM7 or higher with orders of magnitude variation in oil viscosities. Two oil groups (I and II) exactly corresponding to the western and eastern Chepaizi Uplift were distinguished according to their source diagnose. Furthermore, three oil families (II_1, II_2 and II_3), with the biodegradation level of PM7, PM8–8+, PM9+, respectively, were classified based on molecular compositions and parameter-stripping method of strongly bioresistant parameters. Allowing for this extremely high biodegradation case, more biodegradation refractory compound class were added to establish a refined Manco scale to quantitatively evaluate the biodegradation extent. Refined Manco number (RMN_2) positively correlated with the oil density, NSO contents, and absolute concentrations of diasteranes and gammacerane, negatively correlated with the absolute concentrations of diahopane, summed tricyclic terpanes and pentacyclic terpanes. This refined scale showed higher resolution than the PM one to differentiate the biodegradation extent of Carboniferous heavy oils from the Chepaizi Uplift, especially those with same PM values but different oil viscosities.

Keywords Super heavy oil · Biodegradation · Parameter-striping method · Refined Manco scale · Junggar Basin

1 Introduction

Heavy oil and oil sand bitumen dominate the world's oil inventory (Marcano et al. 2013), even exceed the normal oil in quantity (Wang et al. 2016; Li and Huang 2020). Biodegradation may be responsible for these unconventional resources, which primarily formed from the microbial degradation of the conventional oils over geological timescales (Larter et al. 2012). With the proceeding of biodegradation, the oil will exhibit decreases in mass and net volume, increases in oil density, oil viscosity, oil acidity and sulfur content, enrichments in nitrogen, sulfur and oxygen-containing organic compounds, and trace mental elements, which heavily affect the oil's chemical compositions and physical properties (Larter et al. 2006; Zhou et al. 2008; Forsythe et al. 2019). Even within a single petroleum reservoir, biodegradation may create orders of magnitude variation in oil viscosity and fluid property laterally and vertically (Adams et al. 2012). Allowing for their great impact on the economic value and predictability, knowledge of the petroleum biodegradation is critical in selecting exploitation strategies (Marcano et al. 2013; Yin et al. 2013), evaluating the altering extent (Bautista et al. 2015) and forecasting the oil compositional characteristics and viscosity (Larter et al. 2012; Zhang et al. 2014a, b).

Experimental examinations and case studies indicate that relative sensitivity to microbial attack exist among different compound class, even among the individual compound

Edited by Jie Hao and Chun-Yan Tang

✉ Xiang-Chun Chang
xcchang@sina.com

[1] College of Earth Science and Engineering, Shandong University of Science and Technology, Qingdao 266590, China

[2] Laboratory for Marine Mineral Resources, Pilot National Laboratory for Marine Science and Technology, Qingdao 266071, China

[3] Research Institute of Petroleum Exploration and Development, Shengli Oil Company, Sinopec, Dongying 257001, China

Published online: 23 January 2021

in each class. Therefore, biodegradation is a quasi-stepwise process with consume of biomarkers in a preferential order (Peters et al. 2005). Based on the alteration/removal of saturated biomarkers, i.e., normal alkanes, acyclic isoprenoids, terpanes and steranes, and selected aromatic compounds (mainly aromatic steroids), Peters and Moldowan (1993) developed a classical scale to assess the extent of oil biodegradation, which is typically abbreviated as PM scale. Five terms, i.e., light (PM1–3), moderate (PM4–5), heavy (PM6–7), very heavy (PM8–9) and severe (PM10) are assigned to ranges of the PM scale. Another scheme was established by Wenger et al. (2002) fundamentally based on the alteration extent with a compound class and the presence or depletion of single key compound class, only with the terms of heavy and severe to describe the PM 4–10 range.

The normal alkanes are generally more susceptible to biodegradation than the branched alkanes and isoprenoids (Chen et al. 2017), thus ratios of i-C_5/n-C_5, pristane/n-C_{17} and phytane/n-C_{18} are widely used to assess the alteration content of light to moderate biodegraded oils (Peters and Moldowan 1993). However, some case studies showed no evident correlations between Ph/n-C_{18} and oil API, and then the parameter "mean degradative loss" was proposed to assess the biodegradation extent by means of quantifying the depletion in volumetrically important individual oil constituents, especially for the light to moderate level of alteration (Elias et al. 2007). Additionally, the production and biodegradation of oxygen-containing compounds also follow a preferential order, thereafter the acyclic (DBE 1)/cyclic (DBE 2-4) can reveal the biodegradation level, which well correlated with the PM scale when it less than PM < 6 (Angolini et al. 2015).

Many case investigations suggest that the sequential microbial degradation of oil constitutes does not occur in a true stepwise fashion and strictly follow the schemes previously developed (Bennett and Larter 2008; Wang et al. 2013; Chang et al. 2018). All these scales are unsuitable for heavy oil or super heavy oil, and for the mixtures of oils (Larter et al. 2012; Zhang et al. 2014a, b). Selecting 8 compound classes (alkyl toluenes, $C_{0\text{-}1}$ naphthalenes, C_2 naphthalenes, C_3 naphthalenes, methyl dibenzothiophenes, C_4 naphthalenes, $C_{0\text{-}2}$ phenanthrenes and steranes) to reflect the increasing resistance to biodegradation, assigning 0–4 scores to describe the removal extent, Larter et al. (2012) proposed a Manco scale to assess the biodegradation level (PM4–8), with its MN2 value positively correlates with oil viscosity, and effectively used (López 2014).

Till now, published studies mainly focused on the geochemical behaviors of molecular biomarkers at the biodegradation level of PM8 or less, for those biodegradation level higher than PM8, rare studies were reported. With the reduction in conventional resources, extremely biodegraded oils continuously discovered in the petroleum exploration attracted much more attention. Using semi-quantitative parameter-stripping method and refined Manco scale, this paper aims to deeply understand and quantitatively determine the biodegradation extent of heavy oils in the Chepaizi Uplift, Junggar Basin, NW China.

2 Geological setting

The Chepaizi Uplift, covering an area of 10,500 km^2, is a petroliferous target of the northwestern Junggar Basin (Zhao et al. 2019), which is surrounded by two hydrocarbon generative source kitchens, i.e., the Changji Sag to the east and Sikeshu sag to the south (Fig. 1). The early stage of late Hercynian tectonic movement witnessed the formation of prototype of the Chepaizi Uplift, which subsequently experienced the intense uplift during the Indosinian and Yanshan movements, slow subsidence during the Himalayan tectonic movement. As an inherited paleo-uplift, Chepaizi Uplift was characterized by the seriously lack of deposition succession in the structurally high parts, with the Cretaceous, Paleogene, Neogene and Quaternary sedimentary rocks overly Carboniferous volcanics (Song et al. 2007).

Due to the multi-staged transgression and uplifting, three sets of favorable reservoir rocks were developed in the Chepaizi Uplift, i.e., medium-fine sandstone and glutenite occurred in the Neogene Shawan Formation, fine sandstones and siltstone occurred in the Cretaceous interval, and basalt, andesite, tuff and volcanic breccia in the Carboniferous interval.

The Hongche Fault, an active fault separating the Chepaizi Uplift from the Changji Sag (Dong et al. 2017; Ni et al. 2019), cut through sandbodies developed in the Cretaceous, Neogene Shawan Formation and volcanics in the Carboniferous, providing a favorable vertical conduit for the migration of hydrocarbon generated in the Changji Sag to the Chepaizi Uplift and yielding three vertical oil-bearing intervals (Miao et al. 2015; Meng et al. 2016).

3 Samples and experimental

3.1 Sample preparation

Eleven DST oil samples from the Carboniferous volcanic interval were collected from wells in the Chepaizi Uplift for geochemical analysis. Asphaltenes were removed from the oil samples and source rocks using n-hexane precipitation, and the deasphaltened oil was divided into two aliquots. The first of these underwent column chromatography using a routine silica gel and alumina column from which aliphatic and aromatic fractions were obtained using n-hexane and dichloromethane (DCM).

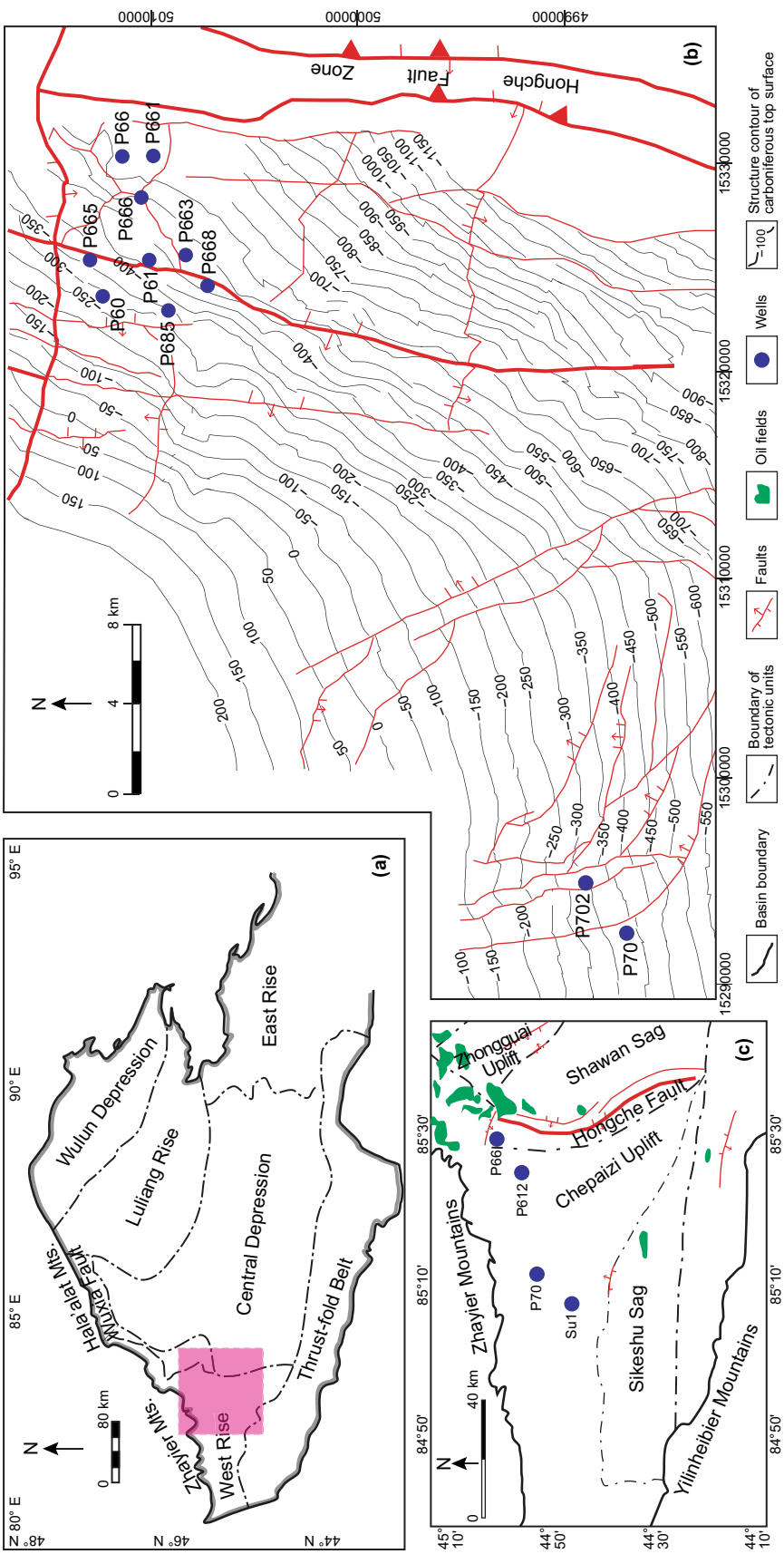

Fig. 1 Map showing structural elements of the Junggar Basin (**a**), with location of the Chepaizi Uplift (**b**), and a field-scale map showing the sampling wells in the Chepaizi Uplift (**c**). This figure was modified after (Chang et al. 2018)

3.2 Gas chromatography–mass spectrometry

Gas chromatography–mass spectrometry (GC–MS) analysis of the aliphatic and aromatic fractions was performed with a Finnigan Model SSQ-710 quadrupole analytical system coupled to a DB-5 fused silica column (30 m × 0.32 mm i.d.) and linked to an IAIS data processing system. GC temperature operating conditions for the aliphatic fraction were as follows: 100 °C (1 min) to 220 °C at 4 °C/min and, then to 300 °C (held 5 min) at 2 °C/min; for the aromatic fraction: 80 °C (1 min) to 300 °C (held 15 min) at 3 °C/min. MS conditions were as follows: electron impact (EI) ionization mode; 70-eV electron energy; 300-mA emission current; and 50–550 amu/s scan range.

4 Results and discussion

4.1 Oil bulk compositions and oil families

The Carboniferous oils from the eastern Chepaizi Uplift are characterized by higher oil density (0.9285–0.9590 g/cm^3) and viscosity (154–8968 mPa·s) than those from the western Chepaizi Uplift, which can be classified as heavy crude oils (Table 1). The Carboniferous oils are predominantly aliphatic, as indicated by their saturate/aromatic (ST/AR) ratio (1.92–3.56) and saturate fraction abundance (44.45%–64.38%). The oil density showed roughly positive correlation with the viscosity and the NSO (resin + asphaltene) fraction content, and negative correlation with the burial depth. Progressive biodegradation of crude oils may be responsible, as it decreases the content of saturate and aromatic hydrocarbons and enriches the resins and asphaltenes, resulting in an increase in oil density (López et al. 2015; Wenger et al. 2002).

As for the study of oil origins, oil family is a widely used term to distinguish oils with different genetic affinity. An oil family, a group of oils that derived from a same source rock, possibly experienced similar reservoir-forming history, belonged to a same oil system, and possessed same or similar chemical compositions. Combing the ratios of C_{27} diasterane 20S/20R (C_{27}DS 20S/20R), C_{27} diasterane/C_{27} regular sterane (C_{27}DS/C_{27}RS), C_{26}/C_{28}triaromatic steroid (20S) (C_{26}/C_{28}TAS(20S)), and C_{27}/C_{28}TAS(20R) with the stable carbon isotope distribution, previous studies concluded that the Carboniferous oils in the eastern Chepaizi Uplift were mainly derived from the mudstone of the Middle Permian Wuerhe Formation (P_2w) in the Changji Sag, whereas the ones in the western Chepaizi Uplift were essentially originated from the Jurassic mudstone in the Sikeshu Sag (Zhang et al. 2012; Xu et al. 2018; Mao et al. 2020). Although two oil charging episodes were defined in the Carboniferous reservoirs based on the oil geochemistry, fluid inclusions and basin modeling (Chang et al. 2019; Shi et al. 2020), the later charge actually was the remigration of early reservoired oils due to the tectonic adjustment (Cao et al. 2010; Song et al. 2016; Chang et al. 2019). Although the Carboniferous oils all exhibited the characteristics of lacustrine source facies, source-diagnostic and redox potential of depositional environment-related molecular biomarkers showed marked distinction between the eastern and western parts (Xu et al. 2018), implying at least two oil groups.

Cluster analysis, a statistical method, is an effective tool to classify studied samples into different groups by their similarity distances which were calculated from the different variables investigated. Allowing for the severe oil alteration, eight biomarker parameters strongly resistant to biodegradation were selected to act as the variables in the clustering analysis, i.e., C_{26}/C_{28}TAS (20S), C_{27}/C_{28}TAS (20R), C_{24} tetracyclic terpane/C_{30} hopane (C_{24}Tet/C_{30}H), gammacerane/

Table 1 Bulk compositions of crude oils from Chepaizi Uplift. ST, saturate hydrocarbon; AR, aromatic hydrocarbon; NSO, resin + asphaltene; G/C_{30}H, gammacerane/C_{30} hopane; *, data cited from Chang et al. (2018) and Xu et al. (2018)

Area	Well	Depth, m	Strata	Density*, g/cm^3	Viscosity*, mPa·s	ST*, %	AR*, %	NSO*, %	δ^{13}C*, ‰	G/C_{30}H*
Western	P70	699–713	C	0.9190	38.5	59.94	12.28	27.78	− 27.50	0.08
	P702	663.7–698.69	C	0.9254	47.1				− 27.80	
Eastern	P66	1109.06–1123.	C	0.9285	154	64.38	18.49	17.12	− 30.40	0.49
	P661	1106.2–1125.0	C	0.9288	149	63.02	20.71	16.27	− 30.00	0.54
	P666	922.69–1140.77	C	0.9297	359	61.40	21.58	17.02	− 29.90	0.51
	P61	855.73–949.58	C	0.9398	390	56.58	17.37	26.05	− 30.10	0.63
	P663	928.45–1031	C	0.9528	1182	55.59	20.68	23.73	− 30.40	0.65
	P668	953.15–1069.51	C	0.9528	1880	44.45	12.50	43.05	− 30.30	0.41
	P60	690–800	C	0.9389	3079	47.06	18.00	34.94	− 31.00	0.66
	P665	781.5–985.85	C	0.9590	8968	45.19	23.01	31.80	− 30.50	3.93
	P685	808.82–892	C	0.9524	2600	47.22	24.60	28.18	− 30.40	4.27

C_{30} hopane (G/C_{30}H), C_{35}H (22S)/C_{34}H (22S), C_{29} 18α(H)-30- norneohopane/C_{29} Hopane (C_{29}Ts/C_{29}H), C_{24} tricyclic terpane (TT)/C_{23}TT, C_{22}TT/C_{21}TT. In the clustering tree graph (Fig. 2), the Carboniferous oils can be clearly divided into two groups, that is, Group I for the western Chepaizi Uplift, Group II for the eastern Chepaizi Uplift. In addition, within the Groups II, three oils families can be further subdivided (II_1, II_2 and II_3) according to their similarity distances.

4.2 Biodegradation level by PM scale

4.2.1 Qualitative evaluation by molecular compositions

1. Oil Group I

Group I (wells P70 and 702), Carboniferous oils from the western Chepaizi Uplift, was least biodegraded among the investigated oils. These oils showed faintly "UCM" and relatively intact *n*-alkanes on the TIC chromatogram (Fig. 3a). Hopanes were slightly higher than the tricyclic terpanes (TTs) in abundance with C_{30} hopane as the peak compound and reversed "L" -shaped distribution of C_{20}TT-C_{21}TT-C_{23} TT (Fig. 3b). Gammacerane (G) was low in content as evidenced by the quietly low G/C_{30}H values (0.08–0.09). Fully developed 25-norhopanes were detected indicating heavy biodegradation. Pregnane, homopregnane, and diasteranes (DS) were lower than the regular steranes (RS) in abundance with "V"-shaped distribution of ααα20R C_{27}-C_{28}-C_{29} steranes (Fig. 3c). Stable carbon isotope varied from −27.5 ‰ ~ −27.8 ‰ (Table 1). Naphthalenes and phenanthrenes were nearly intact and triaromatic steroids (TAS) were essentially unchanged (Fig. 3d). Thereby, Group I can be assigned to biodegradation level of PM6.

2. Oil group II- family II_1

Family II_1 (wells P661, P666 and P66), featured substantially removed *n*-alkanes and *iso*-alkanes and prominent "UCM" on the TIC chromatograms (Fig. 4a). $C_{31–35}$ homohopanes were heavily depleted. Tricyclic terpanes were far higher than hopanes in abundance with reversed "V" distribution of C_{20}TT–C_{21}TT–C_{23}TT (Fig. 4b). Gammacerane was relatively high in content as showed by the high G/C_{30}H values (0.49–0.54). Pregnane and homopregnane were enriched and nearly equal to the regular steranes in abundance with reversed "L" distribution of ααα20R C_{27}–C_{28}–C_{29} sterane (Fig. 4c). Stable carbon isotope varied from −29.9‰ to −30.0 ‰ (Table 1). Naphthalenes and phenanthrenes were substantially depleted (Fig. 4d). The biodegradation can be classified into PM6 + to PM7.

3. Oil group II- family II_2

Family II_2 (wells P663, P668, P61 and P60), showed heavily removed hopane series with C_{29} hopane as the peak compound, equal tricyclic terpanes to hopanes in abundance with sequentially increased distribution of C_{20}TT–C_{21}TT–C_{23} TT (Fig. 5b), and high G/C_{30}H ratios (0.41–0.66). Pregnane and homopregnane far exceeded the regular steranes with "L" distribution of ααα20R C_{27}–C_{28}–C_{29} sterane (Fig. 5c). The diasteranes were prominently altered. Stable carbon

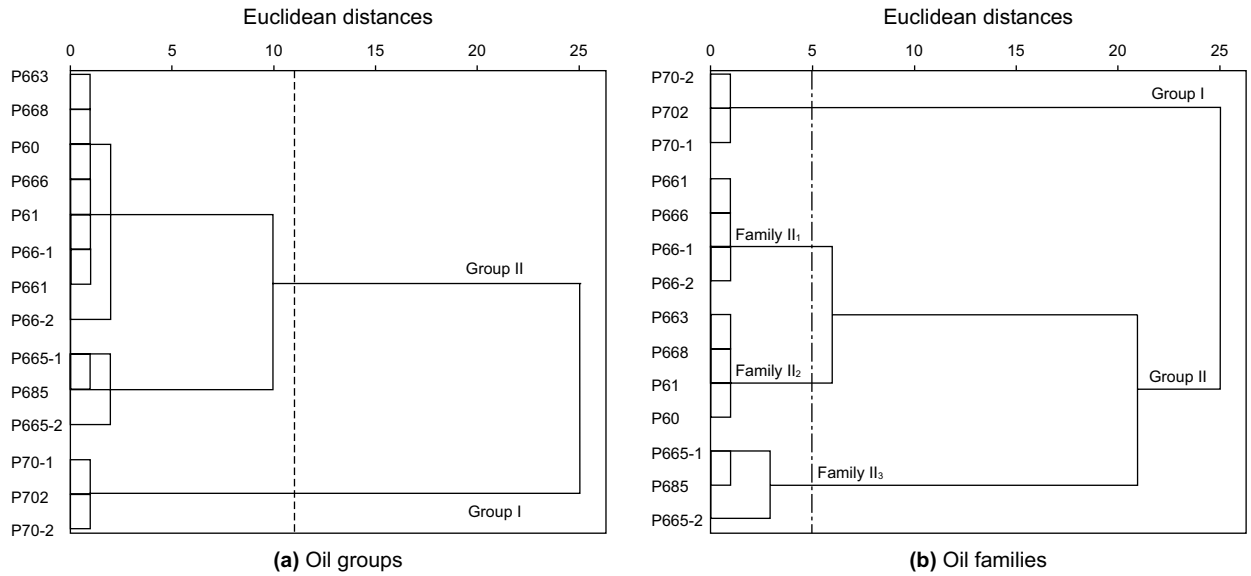

Fig. 2 Clustering tree graphs showing the different oil groups (**a**) and oil families (**b**)

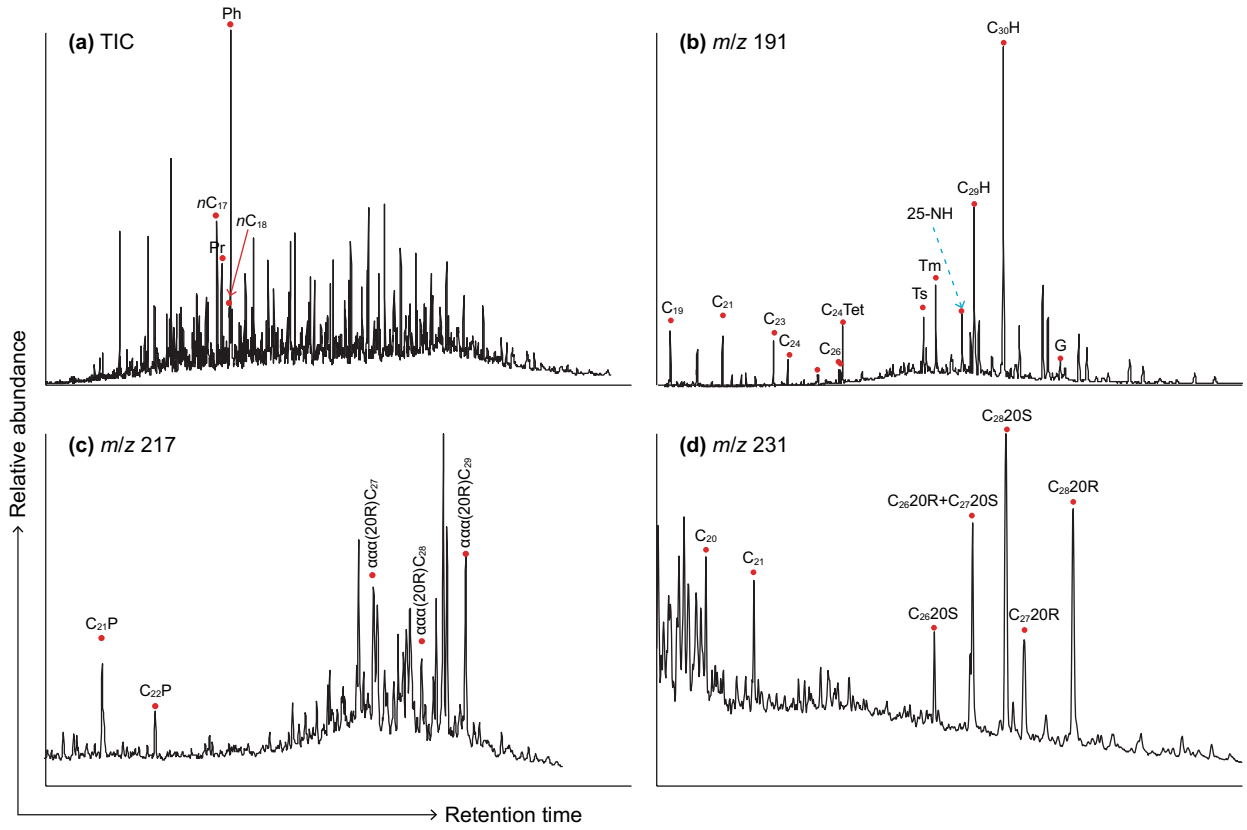

Fig. 3 Representative fragmentograms of oil group I showing molecular compositions (well P70). **a** Total ion chromatogram (TIC); Pr, pristane; Ph, phytane. **b** *m/z* 191, C_{19}-C_{26}, tricyclic terpanes with different carbon number; Tet, tetracyclic terpane; Ts, 18α(H)- trisnorneohopane; Tm, 17α(H)- trisnorhopane; 25-NH, C_{29} 25-norhopane; C_{29}H, C_{29} hopane; C_{30}H, C_{30} hopane; G, gammacerane. **c** *m/z* 217, C_{21}P, C_{21} pregnane; C_{22}P, C_{22} homopregnane; and **d** *m/z* 231, C_{20}–C_{21}, C_{20}–C_{21} triaromatic steroids; C_{26}–C_{28} 20S and 20R,20S and 20R isomers for triaromatic steroids with different carbon numbers

isotope (−29.7‰ to −30.7‰) was like that of the family II_1 (Table 1). Triaromatic steroids were still unchanged (Fig. 5d). The biodegradation level reached PM8 to PM8+.

4. Oil group II- family II_3

Family II_3 (wells P665 and P685), by contrast, exhibited the strongest biodegradation characteristics. Hopanes were essentially removed with C_{29}25-norhopane as the peak compound, and tricyclic terpanes were prominently reduced (Fig. 6b). Gammacerane was abnormally high with G/C_{30}H values ranging from 3.93–4.27. Pregnane and homopregnane were far beyond the majorly depleted regular steranes (Fig. 6c). However, no changes of the stable carbon isotope (−29.7‰ to −30.7‰) can be seen (Table 1). The essentially unaltered triaromatic steroids (Fig. 6d) confirmed the biodegradation level of PM9+.

5. Sequential biodegradation revealed by biomarkers

Although many studies reported that the microbial degradation of oil did not appear to be strictly consistent with the stepwise fashion in established schemes, relative variations of biomarkers in oil families II_1, II_2 and II_3 can be prominently distinguished (Fig. 7). The values of $C_{22}T/C_{21}TT$, $C_{24}TT/C_{23}TT$, $C_{24}C_{24}Tet/C_{26}TT$ and $(C_{20}+C_{21})/C_{26}TT$ ratios increased with the biodegradation extent increased from PM7 to PM8 and finally to PM9+ (Fig. 7a–d), suggesting the alterations of tricyclic terpanes, preferential removal of lower molecular weight homologues and more bioresistance of tetracyclic terpane (Huang and Li 2017). Hopane/sterane ratio varied with biodegradation in a zigzag-shaped fashion (Fig. 7e), i.e., essentially unchanged from the level of PM6+ to PM7, sharply increased from the level of PM7 to PM8, and progressively decreased from the level of PM8 to PM9+, confirming the different susceptibility to biodegradation for hopanes and steranes at different biodegradation level (Reed 1977;). Ratios of C_{29}/C_{30}H, G/$_{30}$H and C_{30} diahopane/C_{30} hopane (C_{30}D/C_{30}H) kept relatively unchanged from level PM7 to PM8, then sharply increased to PM9+ (Fig. 7f–h), indicating approximately

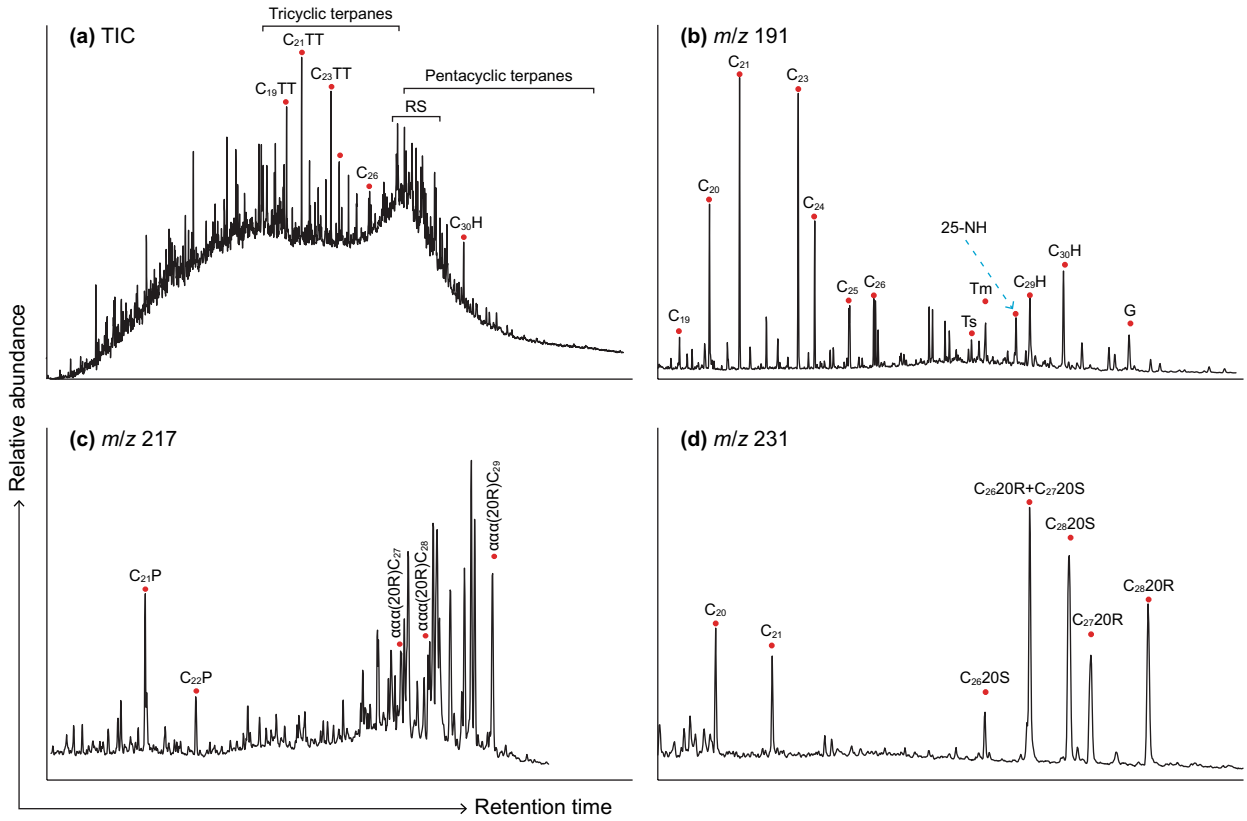

Fig. 4 Representative fragmentograms of oil family II_1 showing molecular compositions (well P661). **a** Total ion chromatogram (TIC), RS, regular sterane, **b** *m/z* 191, **c** *m/z* 217, and **d** *m/z* 231. Abbreviations are the same to Fig. 3

the same bioresistance of C_{30} hopane to C_{29} hopane, gammacerane and C_{30} diahopane before PM8 level, but more susceptibility at level PM9+. Gradually increased 18α(H)-trisnorneohopane/17α(H)- trisnorhopane (Ts/Tm) ratio with biodegradation indicated the relatively more susceptible of Tm than Ts to microbial alteration (Fig. 7i). Increasing C_{29} 25-norhopane/gammacerane (C_{29}NH/G) value with biodegradation confirmed the formation of 25-norhopane (Fig. 7j) at level above PM6, which was consistent with the increasing C_{28}NH/C_{29}H and C_{29}NH/C_{30}H (Fig. 7k, 7l). However, its decrease from PM8 to PM9+revealed the degradation of 25-norhopanes occurred under extreme biodegradation level (Huang and Li 2017; Chang et al. 2018; Killops et al. 2019), as validated by the increasing C_{29}NH/C_{28}NH (Fig. 7m). 25-norhopane ratio ($\sum C_{30}$–C_{34} 25-norhopanes/($\sum C_{30}$–C_{34} 25-norhopanes + $\sum C_{31}$–C_{35} homohopanes) generally exhibited a tendency to be increased with biodegradation, which was consistent with the formation of 25-norhopanes and reduction in homohopanes (Fig. 7n). Increasing C_{27}DS/C_{27}RS with biodegradation displayed the faster degradation of regular steranes than the diasteranes after PM7 level (Fig. 7o). Unchanged C_{26}/C_{28}TAS(20S) and C_{27}/C_{28}TAS(20R) well documented the strongest bioresistance of triaromatic steroids (Fig. 7q, 7r), yet the decreasing ($C_{20}+C_{21}$)/C_{26-28}TAS demonstrated that the short-chained counterparts were slightly destroyed above PM7 (Fig. 7p).

4.2.2 Semi-quantitative evaluation by parameter-stripping method

Ideally, biomarkers were sequentially removed by biodegradation in a stepwise fashion and can be described by the ten-point scales (Peters and Moldowan 1993). To further proof the extent of biodegradation four biodegradation stages were defined following the general alteration tendency in PM scheme (Fig. 8). Stage 1 covers approximately from PM1 to PM5, stage 2 from PM5 to PM7, stage 3 from PM7 to PM8, and stage 4 involves PM8 and higher. Biodegradation levels of different oil families were semi-quantitatively defined by sequentially stripping the samples in the cross-plots of biodegradation-resistant parameters.

1. Stage 4

Diasteranes show particular resistance to biodegradation and remain where steranes and hopanes are totally removed in case of no 25-norhopanes are present (PM9) (Peters et al.

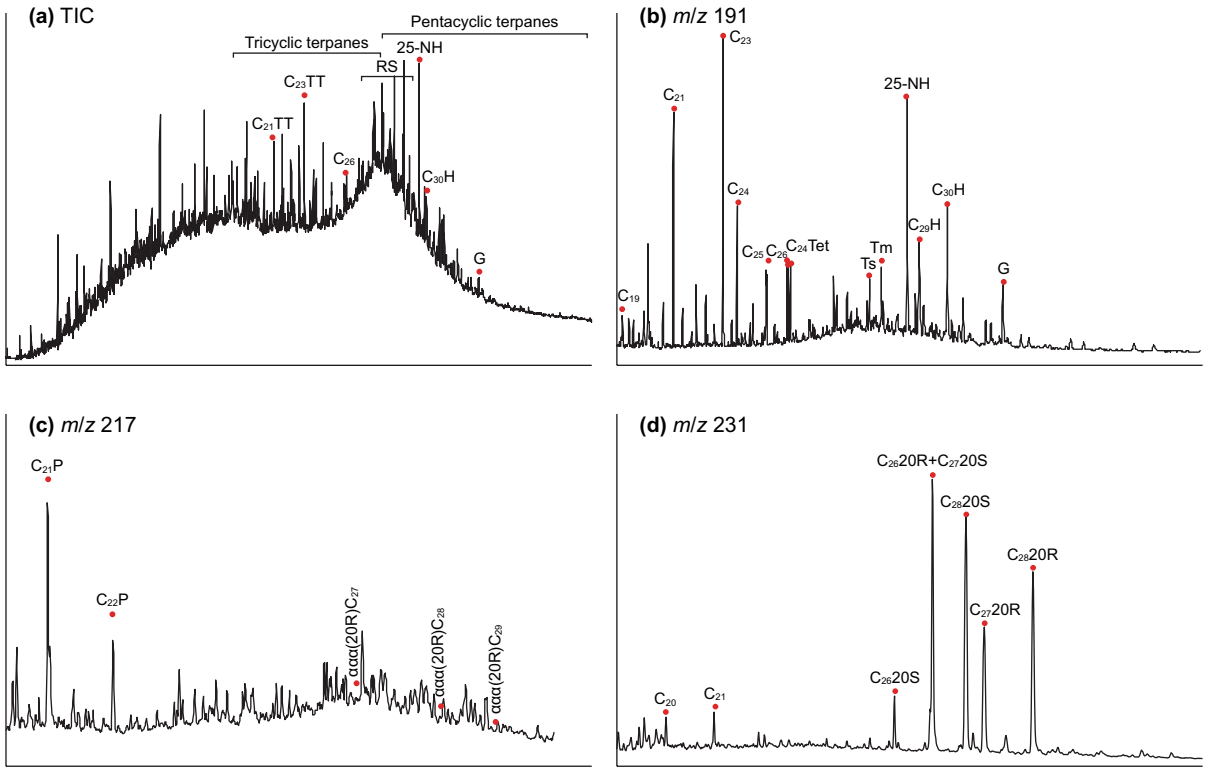

Fig. 5 Representative fragmentograms of oil family II_2 showing molecular compositions (well P663). **a** Total ion chromatogram (TIC), **b** *m/z* 191, **c** *m/z* 217, and **d** *m/z* 23. All abbreviations are the same to Fig. 3

2005). Pregnane (P) and homopregnane have high resistance to biodegradation, comparable to the diasterane (PM9). Tricyclic terpanes can be altered at about the same level as the diasteranes (Lin et al. 1989). Non-hopanoid triterpanes, such as gammacerane, diahopanes, oleanane, are highly resistant to biodegradation (Peters et al. 2005), and even beyond the point (PM ≥ 9) where the tricyclic terpanes have been removed (Wenger and Isaksen 2002). Although aromatized steroids keep unaltered in all but the most severely biodegraded oils (PM10) and can be effectively used to determine the origin and thermal maturity for extremely biodegraded oils (Peters and Moldowan 1993), low molecular weight triaromatic steroids (C_{20}-C_{21}) are among the first aromatic steroids to be depleted during biodegradation (Wardroper et al., 1984). From the cross-plots of gammacerane/C_{30} diahopane (G/C_{30}D) vs. C_{27}DS(20S)/C_{27}DS(20R), C_{26}/C_{28}TAS(20S) vs. C_{27}/C_{28}TAS(20R), Carboniferous oils in the western and eastern Chepaizi Uplift were clearly distinguished exactly corresponding to the Group I and II, respectively (Fig. 9a, 9b).

Using triaromatic steroids ratios, previous studies concluded that the Carboniferous oils from the eastern Chepaizi Uplift had a common origin and similar maturities (Xi et al. 2014; Xiao et al. 2014; Xu et al. 2018; Chang et al. 2019; Mao et al. 2020); therefore, the biodegradation extent may be responsible for the observed differences of oil compositions. The tricyclic terpanes feature similarly high bioresistance to the diasteranes (PM > 8; Lin et al. 1989), slightly lower than the non-hopanoid terpanes. In the extreme biodegradation cases, tricyclic terpanes with lower molecular weight would be preferentially degraded (Huang and Li 2017; Chang et al. 2018). Oil family II_3 exhibited prominently higher C_{24}/C_{23}TT and C_{22}/C_{21}TT ratios than other oil families, implying a biodegradation level at least up to PM 9–PM9+ (Fig. 9c). Obviously, by contrast, the biodegradation rank of family II_1 and II_2 were lower than PM9.

2. Stage 3

Hopanes are removed before or after steranes, 25-norhopanes occur in oils where the hopanes are preferentially removed (Reed 1977; Peters et al. 2005), as supported by this investigation (Fig. 7e). C_{31} and C_{32} homohopanes were more susceptible to biodegradation than C_{30} hopane in the asphalts from Madagascar (Rullkotter and Wendisch 1982), while C_{28}-C_{30} 17α-hopanes are typically biodegraded in the same manner and at approximately the same rate as the C_{31}-C_{35} extended hopanes (Williams et al. 1986). The 25-norhopane ratio, that is ratio of the total C_{30}–C_{34}

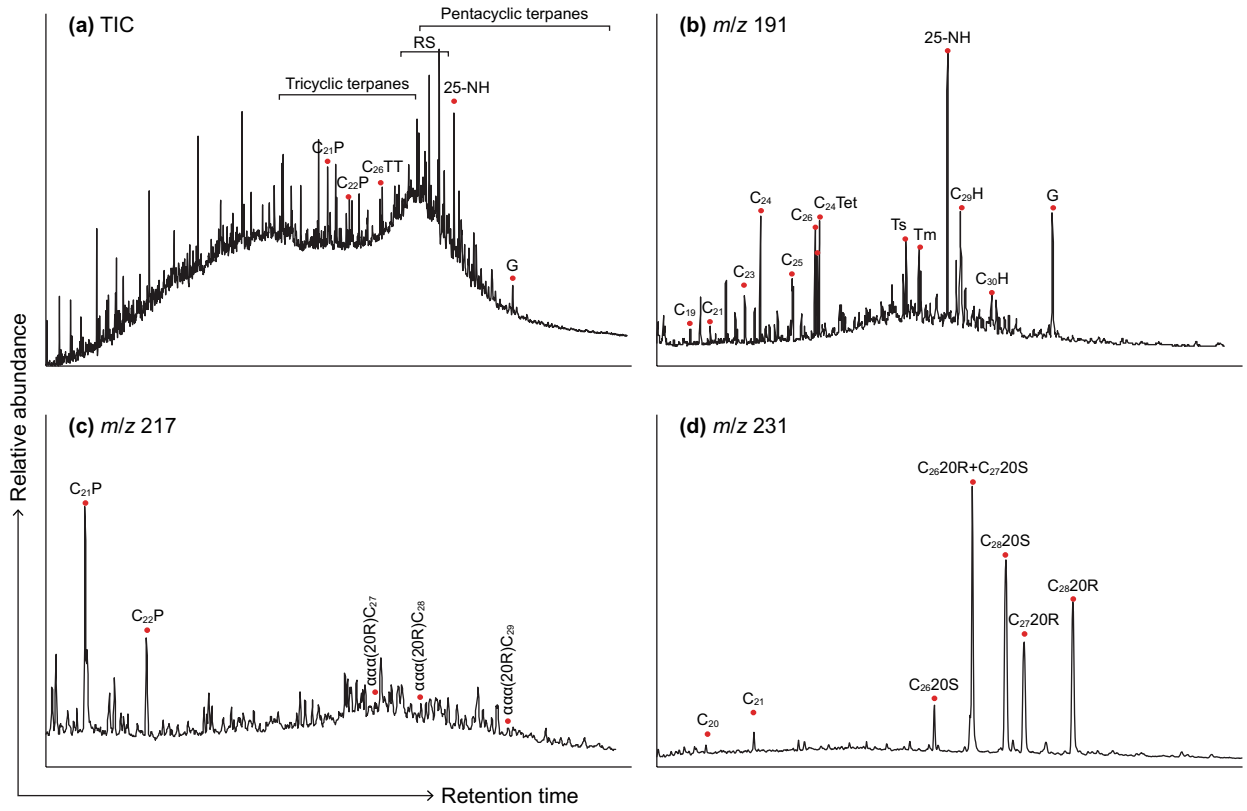

Fig. 6 Representative fragmentograms of oil family II_3 showing molecular compositions (well P665). **a** Total ion chromatogram (TIC), **b** *m/z* 191, **c** *m/z* 217, and **d** *m/z* 23. All abbreviations are the same to Fig. 3

25-norhopanes to the sum of these compounds plus the C_{31}–C_{35} homohopanes, could be used to evaluate the alternation extent among severely biodegraded oils of PM ~ 6–9 (Peters et al. 1996). Oil family II_2, featured medium ratios of C_{21} P/$\sum C_{27-29}$ RS and C_{22} P/$\sum C_{27-29}$ RS (Fig. 9d), which clearly distinguished from those of the family II_3 (quite high) and family II_1 (rather low), and further verified by the varying range of C_{29}25-NH/C_{30}H and C_{30}25-NH/C_{31}H ratios (Fig. 9e). Hence, the biodegradation level of the family II_2 can be evaluated at PM8–PM8+, while the family II_1 less than PM8.

3. Stage 2

Normal alkanes are preferentially removed at the biodegradation level of PM1–2; however, selective biodegradation of the isoprenoid over more bioresistant steranes or hopanes is used to determine the level of PM3–4 (Peters et al. 2005). Long-chained alkylated cyclopentanes and cyclohexanes are about as susceptible as branched alkanes and monocyclic alkanes will be depleted or in trace quantities at PM3–4 level (Peters and Moldowan 1993). C_{14}-C_{16} bicyclic terpanes are less susceptible to biodegradation than isoprenoid and will be completely eliminated before the start of sterane and hopane biodegradation (Peters et al. 2005). Regular steranes are removed after the complete removal of C_{15}-C_{20} isoprenoids and before or after the hopanes (Peters et al. 2005). Comparatively, slight alteration of methyl and dimethylnapthalenes occurs during the removal of *n*-alkanes, trimethylnaphthalenes are altered during the removal of the isoprenoids, and tetramethylnaphthalenes persist until steranes are largely depleted (Fisher et al. 1998). Phenanthrenes are generally more resistant to biodegradation than alkylnaphthalenes, and methylbiphenyls, dimethylbiphenyls, and methyldiphenylmethanes lacks in the biodegraded oils at PM7 (Peters and Moldowan 1993). Higher-hopane homologues, particularly the C_{35} pentahomohopanes, are preferentially bioresistant, and the alteration of C_{35} homhopanes are possibly at the rank of PM ≥ 7 (Seifert et al. 1984; Moldowan et al. 1995). The G/C_{30}H and C_{29} hopane/C_{30} hopane (C_{29}H/C_{30}H) varied from roughly unchanged to rapidly increased with the increasing biodegradation level, confirming the faster degradation of C_{30}H than C_{29}H, especially at level higher than PM8 (Bennett et al. 2006; Chang et al. 2018); however, the substantial constancy of C_{29} 18α-30-norneohopane/C_{29} hopane (C_{29}Ts/C_{29}H) implies the similar susceptibility of C_{29}Ts and C_{29}H to biodegradation (Chang et al. 2018). Oil family II_3 was biodegraded to PM7

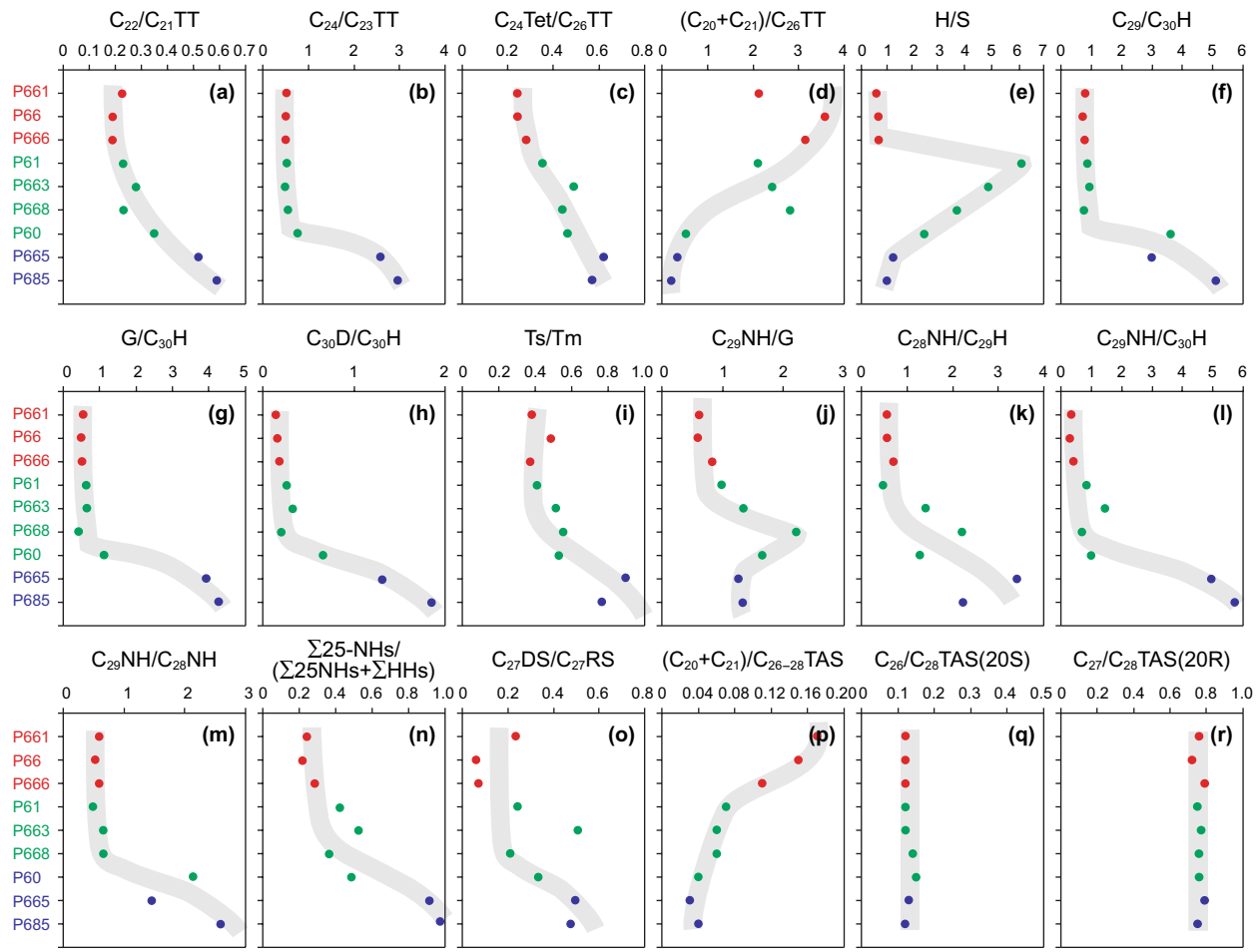

Fig. 7 Correlations of biomarker parameters among three oil families of Group II showing the alterations of biomarkers with different susceptibility to biodegradation. TT, tricyclic terpane; Tet, tetracyclic terpane; H, hopane; G, gammacerane; Ts, 18α(H)-trisnorneohopane; Tm, 17α(H)-trisnorhopane; NH, 25-norhopane; $C_{30}D$, C_{30} diahopane; ∑25-NHs, sum of C_{30}-C_{34} 25-norhopanes; ∑HHs, sum of C_{31}-C_{35} homohopanes; DS, diasterane; RS, regular sterane; TAS, triaromatic steroid. All the ratio data were cited after (Chang et al. 2018)

by its lower C_{35}/C_{34} hopane (22S) and HHI values (Fig. 9f, g). Furthermore, the tetramethylnaphthalene ratio (TeBR = 1,3,6,7-TeMN/1,3,5,7TeMN, TeMN = tetramethylnaphthalene; Peters et al. 2005) begins to be altered significantly at levels PM5–6 (Fisher et al. 1998). Therefore, oil family II_1 distinctly distinguished from other families and showed biodegradation level of PM7 as evidenced by the higher TeBR values (Fig. 9h).

4. Stage 1

No biodegradation occurred.

4.3 Quantitative evaluation by refined Manco scale

4.3.1 Refined Manco scale

The present biodegradation scales are essentially established according to the presence or absence of single compound classes and the alteration extent within a compound class, which encountered issues for super heavy oils (Larter et al. 2012). Manco scale emerged as the requirement, integrating the extent of degradation of various sets of compound classes. This quantitative Manco scale provided a higher resolution, however, only effective for the biodegradation of PM4–8.

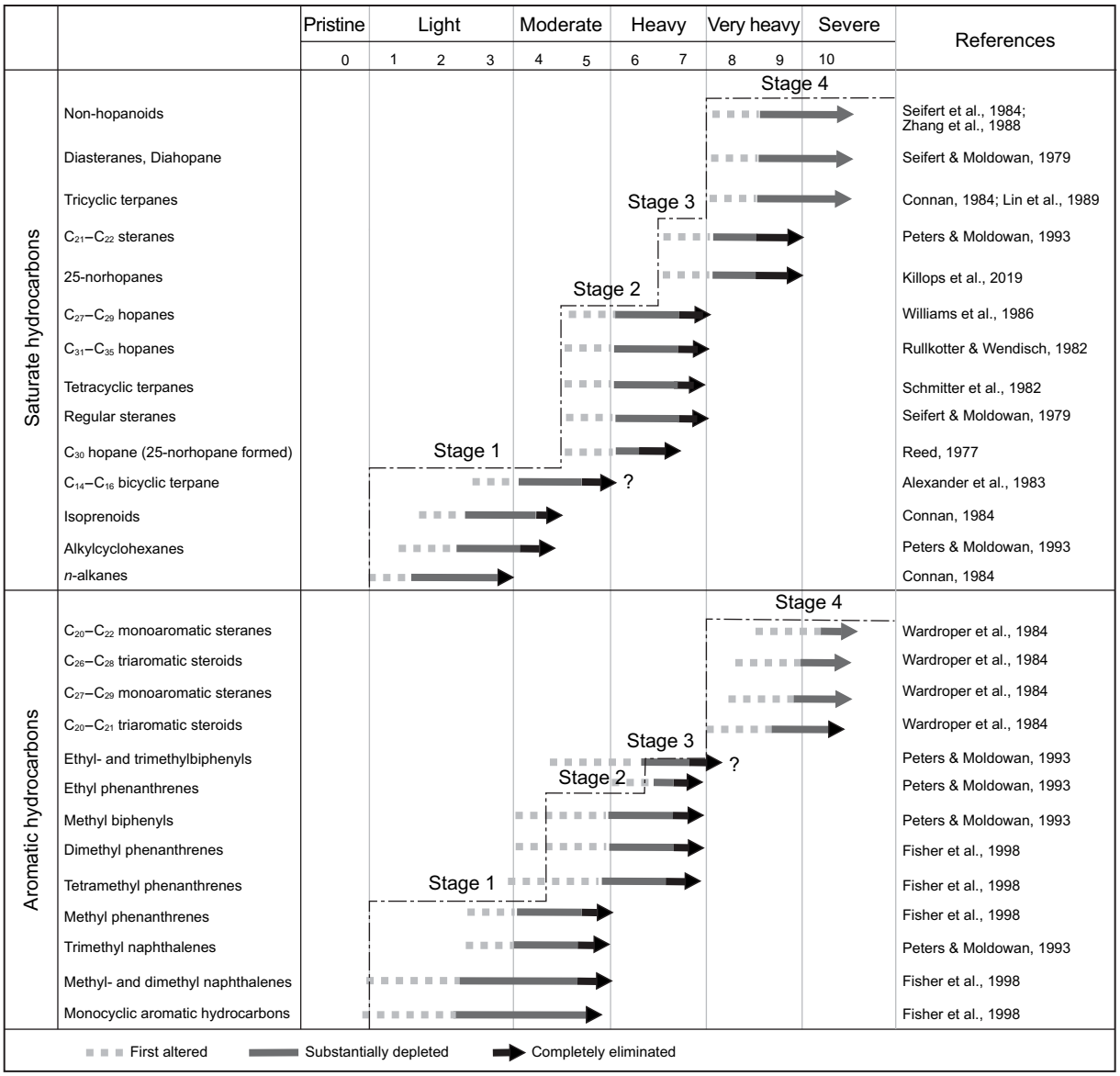

Fig. 8 Schematic plot of the four-stages of the PM scale

More biodegradation refractory compound class, i.e., 25-norhopane, tricyclic terpanes and triaromatic steroids, were added to refine the Manco scale to meet the situation of very heavy to severe biodegraded oils from Chepaizi Uplift. Followed the academic principles of Manco scale, eight compound classes that covered the whole range of biodegradation rank (PM0–10) and possessed increasing resistance to biodegradation were selected as vector elements. The eight compound classes and their GC–MS detection m/z values are listed in Table 2.

Five levels of refined Manco score (RMS) from 0–4 were assigned to the 8 compound classes, referencing after the Manco scale (Table 3). The refined Manco number (RMN_1 and RMN_2) can be calculated by the following formulas.

$$RMN_1 = \sum m_i 5^i$$

$$RMN_2 = [n + (\log_5 (RMN_1) \cdot (S_{\max} - 1)]/n$$

where m refers to the refined Manco score for each out of the eight vector elements (0–4), i means the class number (0–7), and n is the number of compound classes. $S_{\max}$, maximum for RMN_2, is designate to be 1000 to avoid confusion with the currently existing scales, and to ensure enough resolution at different levels of biodegradation when using integer values.

When applied the refined Manco scale to evaluate the Carboniferous oils in the Chepaizi Uplift (Table 4), the

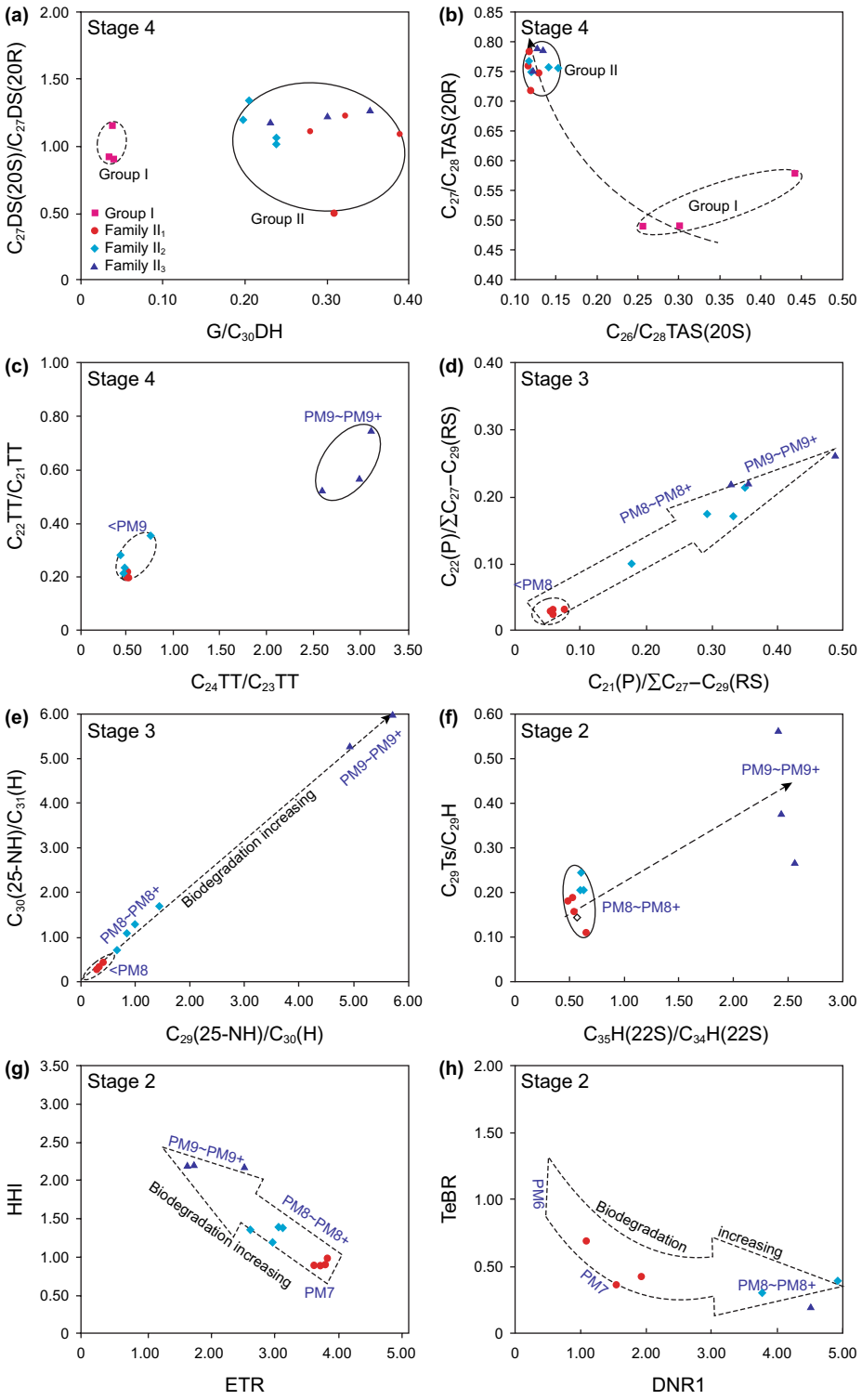

Fig. 9 Scattering plots of the Carboniferous oils by the parameter-striping method. DS, diasterane; G, gammacerane;/DH, diahopane; TAS, triaromatic steroid; TT, tricyclic terpane; P, pregnane; RS, regular sterane; 25-NH, 25-norhopane; H, hopane; C_{29}Ts, C_{29} 18α-30-norneohopane; HHI, C_{35} homohopane/sum of C_{31}-C_{35} homohopanes; ETR, (C_{28} tricyclic terpane + C_{29} tricyclic terpane)/(C_{28} tricyclic terpane + C_{29} tricyclic terpane +18α(H)-trisnorneohopane); TeBR, 1,3,6,7-/1,3,5,7 tetramethylnaphthalene; DNR1, (2,6- +2,7-)/1,5-dimethylnaphthalene; *, data cited from Chang et al. (2018)

Table 2 Refined compound classes used to represent increasing bioresistance

Vector element	Compound class	GC–MS m/z value
0	*n*-alkanes + $C_{1\text{-}4}$ naphthalenes	85 + 156 + 170 + 184 + 198
1	Alkyl dibenzothiophenes	198 + 212 + 226
2	$C_{0\text{-}3}$ phenanthrenes	178 + 192 + 206 + 220
3	C_4 phenanthrenes	234
4	Hopanes + methylhopanes + 25-norhopanes	191 + 177 + 205
5	Regular steranes + diasterane + short-chain sterane	217 + 218 + 259
6	Tricyclic terpanes + 17-nor tricyclic terpane	191 + 177
7	Triaromatic steroid + methyl triaromatic steroid	231 + 245

RMN_2 generally well correlated with the viscosity and NSO content (Fig. 10a, b), implying the loss of oils, especially those light ends or susceptible compounds with increasing biodegradation extent. Summed pentacyclic terpanes (∑PTs), summed tricyclic terpanes (∑TTs) and diasteranes concentrations decreased with the increasing RMN_2 (Fig. 10c, d, f), suggesting the slight alterations of pentacyclic terpanes, tricyclic terpanes and diasteranes from the PM7 to PM8 level, and sharp depletion from PM8 to PM9 + . However, the variation of diahopane concentrations (Fig. 10e) possibly indicated its high bioresistance or other mechanism needed to further investigate.

Generally, RMN_2 ranged from 546.04 to 909.63, which approximately distinguished the oils at the level of PM6 to PM9 + (Table 4). Exceptionally, by contrast, the oils from well P60 exhibited higher oil density but lower biodegradation extent than that from well P685. Factually, there is not a simple relationship between the oil viscosity and the Manco Number (Larter et al. 2012). Processes other than biodegradation, i.e., secondary oil charge, water washing, mixing of multiple maturity oil charges, and loss of light ends from heavy oils could produce variations in oil viscosity and API gravity (López 2014). The two episodes of oil charging, early biodegraded oils mixed with the later remigration of preexisting oils due to the structural adjustment, yet the same oil origin in the Chepaizi Uplift maybe responsible for this case (Chang et al. 2019; Shi et al., 2020).

Notably, although the RMN_2 calculated by the refined Manco scale showed roughly positive correlation with oil density, some samples, especially those three biodegraded at PM8, exhibited much the same RMN_2 but with different oil densities. This indicated that biodegradation refractory compound class added in this refined scale could not perfectly differentiate the appearances among oils biodegraded at about PM8. More assemblages of compound classes need to be established to refine the Manco scales in further trials.

4.4 Geochemical implications

Although the Carboniferous oils in the western and eastern Chepaizi Uplift were derived from different source kitchens, oils within the individual groups had common origin and similar maturities (Zhang et al. 2014a, b; Xi et al. 2014; Xiao et al. 2014; Xu et al. 2018; Mao et al. 2020). The differences observed in PM and refined Manco scales were mainly attributed to the biodegradation extent. By contrast, the refined Manco scale showed higher resolution than the PM scale, which can differentiate the biodegradation extent of super heavy oils with same PM values but different oil viscosities (Table 4).

For the eastern Chepaizi Uplift, Carboniferous oils were mostly biodegraded above PM8; however, their oil viscosity displayed orders of magnitude variations. Known to all, the physical properties, particularly the oil viscosity, were critical to the choice of exploration strategies. Subtle differences revealed by the refined Manco scale could be helpful. Besides the practical application, refined Manco scale also allow geochemists conducting more basic study to understand the relative differences in the extent of the biodegradation process among related samples.

5 Conclusions

The heavy to severe biodegradation was responsible for the Carboniferous heavy oils in the Chepaizi Uplift, with PM6 in the western and PM7–PM9+ in the eastern part, respectively. According the oil-source correlation, the oils in the western Chepaizi Uplift were derived from the Jurassic source rock in the Sikeshu sag and those in the eastern Chepaizi Uplift were originated from the Permian source rocks in the Changji sag. Therefore, two oil groups (I and II) were distinguished. Three oil families (II_1, II_2 and II_3) were subdivided with the biodegradation level of PM7, PM8–8+ , PM9+ , respectively, based on molecular

Table 3 Refined Manco Scores used to qualitatively distinguish the biodegradation level of compound classes

Vector element	Compound class	Refined Manco Scores
0	*n*-alkanes + C_{1-4} naphthalenes	0: intact n-alkanes 1: slightly degraded n-alkanes, C_3 naphthalene as the peak compound of alkyl naphthalenes 2: substantially degraded n-alkane, C_3 naphthalene as the peak compound of alkyl naphthalenes 3: essentially depleted n-alkanes, C_4 naphthalene as the peak compound of alkyl naphthalenes 4: partially remained C_4 naphthalene in the alkyl naphthalenes
1	Alkyl dibenzothiophenes	0: non-degraded 1: only slightly degraded 2: mid-way between the extremes 3: not quite fully degraded 4: typically absent
2	C_{0-3} phenanthrenes	0: complete C_{0-3} phenanthrenes with the C_0 phenanthrene as peak compound 1: slightly degraded phenanthrenes with the C_{1-2} phenanthrene as peak compounds 2: dimethyl and ethyl phenanthrene begun to be altered with the C_2 phenanthrene as peak compound 3: substantially degraded dimethyl and ethyl phenanthrene, C_3 phenanthrene begun to be altered with the C_3 phenanthrene as peak compound 4: wholly removed dimethyl and ethyl phenanthrene, only trace C_3 phenanthrene remained
3	C_4 phenanthrenes	0: non-degraded 1: only slightly degraded 2: mid-way between the extremes 3: not quite fully degraded 4: typically absent
4	Hopanes + methylhopanes + 25-norhopanes	0: intact hopanes with C_{30} hopane as the peak compound 1: hopanes begun to be degraded still with C_{30} hopane as the peak compound, and 25-norhopane was present 2: hopanes were substantially degraded with C_{30} or C_{29} hopane as the peak compound, 25-norhopane was prominently enriched in abundance 3: C_{29}-25norhopane was the peak compound in m/z 191 chromatograms, 25,28-binorhopane begun to come into existing. 4: completely depleted hopanes with C_{29} 25-norhopane as the peak compound, 25,28-binorhopane increased prominently in abundance.
5	Regular steranes + diasterane + short-chain sterane	0: completed regular steranes with higher contents compared to diasteranes 1: slightly degraded regular steranes, slightly lower contents than diasteranes 2: substantially degraded regular steranes, which were evidently lower than the slightly degraded diasteranes 3: essentially depleted regular steranes, substantially degraded diasteranes
6	Tricyclic terpane + 17-nor tricyclic terpane	0: intact TTs 1: slightly degraded TTs with the presence of 17-nor tricyclic terpane 2: substantially degraded TTs with relatively increased 17-nortricyclic terpane 3: essentially degraded TTs, with far higher 1contents of 17-nortricyclic terpane than TTs
7	Triaromatic steroid + methyl triaromatic steroid	0: intact triaromatic steroid and methyl triaromatic steroid 1: slightly degraded C_{19}-C_{20} triaromatic steroids, and unaltered C_{26}-C_{28} triaromatic steroids and methyl triaromatic steroids 2: substantially removed low-carbon-number triaromatic steroids and methyl triaromatic steroids, high-carbon-number triaromatic steroids still unchanged

Table 4 Refined Manco numbers for Carboniferous oils of Chepaizi Uplift calculated by the refined Manco scores. P, pregnane; DH, diahopane

Well	Vector element								RMN_2	PM	DS*, μg/g	G*, μg/g	∑PTs*, μg/g	∑TTs*, μg/g	P*, μg/g	DH*, μg/g
	0	1	2	3	4	5	6	7								
P70	4	4	4	3	1	0	0	0	546.04	6	–	–	–	–	–	–
P702	4	4	4	3	2	0	0	0	580.34	6	–	–	–	–	–	–
P66	4	4	4	3	3	1	0	0	669.22	7	44.96	175.41	1478.11	2596.9	83.42	55.75
P661	4	4	4	4	3	1	0	0	670.97	7	115.02	139.3	1110.92	2825.58	62.29	20.05
P666	4	4	4	4	3	1	0	0	670.97	7	120.37	141.77	1313.7	2465.01	61.97	29.49
P61	4	4	4	4	4	2	1	0	786.71	8	37.05	144.57	1218.28	2140.41	68.76	45.95
P663	4	4	4	4	4	2	1	0	786.71	8	35.14	161.56	1353.03	1525.6	73.84	56.51
P668	4	4	4	4	3	2	1	0	784.45	8	44.04	129.12	1285.58	1452.22	64.23	47.65
P60	4	4	4	4	3	2	1	0	784.35	8+	–	–	–	–	–	–
P665	4	4	4	4	4	3	2	1	909.63	9+	–	–	–	–	–	–
P685	4	4	4	4	4	3	2	0	830.14	9+	27.76	220.18	945.75	780.71	103.28	69.37

compositions and parameter-stripping method of strongly bioresistant parameters. Three biodegradation refractory compound class (25-norhopane, tricyclic terpanes and triaromatic steroids) were added to establish a refined Manco scale to quantify the biodegradation extent of Carboniferous oils from Chepaizi Uplift. The evaluation results clearly differentiate the biodegradation extent of heavy oils with same PM values but different oil viscosities, indicating a high resolution and potential prospect.

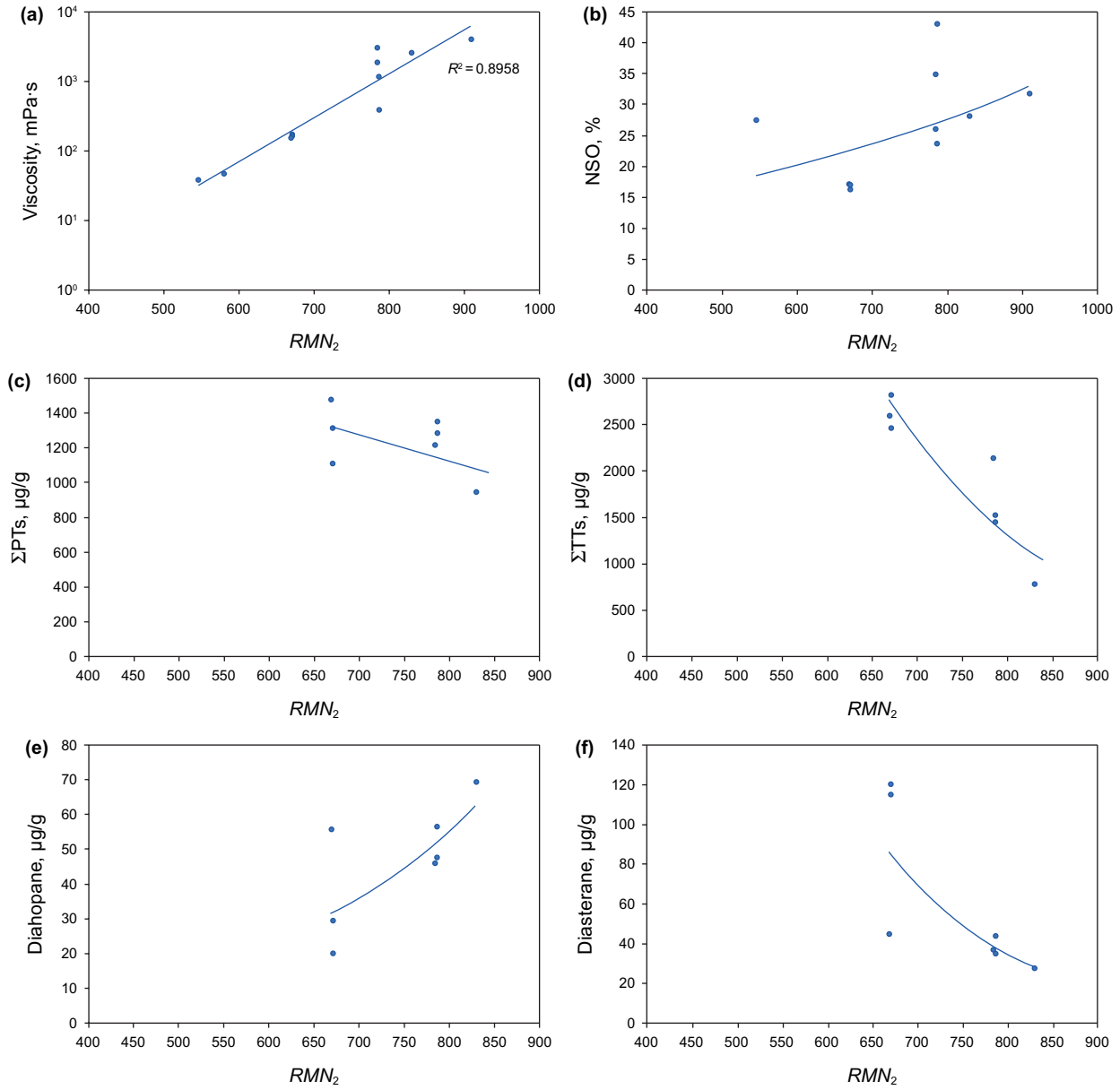

Fig. 10 Correlations of the refined Manco number (MN2) with oil viscosity (**a**), NSO content (**b**), summed pentacyclic terpane (**c**) and tricyclic terpane concentrations (**d**), and absolute concentrations of diahopane (**e**) and diasteranes (**f**). All the concentration data were cited after (Chang et al. 2018)

Acknowledgement This work was funded by the National Natural Science Foundation of China (Grant No. 42072172, 41772120), the Shandong Province Natural Science Fund for Distinguished Young Scholars (Grant No. JQ201311), and the SDUST Research Fund (Grant No. 2015TDJH101). Associated editor Jie Hao and seven anonymous reviewers were deeply acknowledged for their critical comments and helpful suggestions, which greatly improved the early version of this manuscript.

References

Adams JJ, Larter SR, Bennett B, et al. The dynamic interplay of oil mixing, charge timing, and biodegradation in forming the Alberta oil sands: Insights from geologic modeling and biogeochemistry. In: Hein F J, Leckie D, Larter S, et al. (Eds.), Heavy-oil and Oil-sand Petroleum Systems in Alberta and Beyond: AAPG Studies in Geology, 2012; 64: 1–80.

Angolini CFF, Capilla R, Marsaioli J. Petroleum biodegradation effects on polar acidic compounds and correlation with their corresponded hydrocarbon fractions. Energy Fuels. 2015;29:4886–92. https://doi.org/10.1021/acs.energyfuels.5b01116.

Bautista DFC, Santos-Neto EVD, Penteado HLdeB. Controls on petroleum composition in the Llanos basin: implication for exploration. AAPG Bulletin. 2015;99(8):1503–35. https://doi.org/10.1306/10231411111.

Bennett B, Fustic M, Farrimond P, et al. 25-Norhopanes: formation during biodegradation of petroleum in the subsurface. Org Geochem. 2006;37:787–97. https://doi.org/10.1016/j.orggeochem.2006.03.003.

Bennett B, Larter SR. Biodegradation scales: applications and limitations. Org Geochem. 2008;39:1222–8. https://doi.org/10.1016/j.orggeochem.2008.02.023.

Cao J, Jin ZJ, Hu WX, et al. Improved understanding of petroleum migration history in the Hongche fault zone, northwestern Junggar Basin (northwest China): constrained by vein–calcite fluid inclusions and trace elements. Mar Pet Geol. 2010;27:61–8. https://doi.org/10.1016/j.marpetgeo.2009.08.014.

Chang XC, Wang Y, Shi BB, et al. Charging of Carboniferous volcanic reservoirs in the eastern Chepaizi Uplift, Junggar Basin (northwestern China) constrained by oil geochemistry and fluid inclusion. AAPG Bulletin. 2019;103(7):1625–52. https://doi.org/10.1306/12171818041.

Chang XC, Zhao HG, He WX, et al. Improved understanding of the alteration of molecular compositions by severe to extreme biodegradation—a case study from the Carboniferous oils in the eastern Chepaizi Uplift, Junggar Basin, NW China. Energy Fuels. 2018;32(7):7557–68. https://doi.org/10.1021/acs.energyfuels.8b01557.

Chen JP, Deng CP, Wang XL, et al. Formation mechanism of condensates, waxy and heavy oils in the southern margin of Junggar Basin, NW China. Science China Earth Sciences. 2017;60(5):972–91. https://doi.org/10.1007/s11430-016-9027-3.

Dong DW, Li JY, Yang YH, et al. Improvements to the fuzzy mathematics comprehensive quantitative method for evaluating fault sealing. Pet Sci. 2017;14:276–85. https://doi.org/10.1007/s12182-017-0158-1.

Elias R, Vieth A, Riva A, et al. Improved assessment of biodegradation extent and prediction of petroleum quality. Org Geochem. 2007;38:2111–30. https://doi.org/10.1016/j.orggeochem.2007.07.004.

Fisher SJ, Alexander R, Kagi RI, et al. Aromatic hydrocarbons as indicators of biodegradation in north Western Australian reservoirs. In: Sedimentary Basins of Western Australia: West Australian Basins Symposium (P. G. Purcell and R. R. Purcell, eds.), Petroleum Exploration Society of Australia, WA Branch, Perth, Australia, 1998; pp. 185–94.

Forsythe JC, Kenyon-Roberts S, O'Donnell M, et al. Biodegradation and water washing in a spill-fill sequence of oilfields. Fuel. 2019;237:707–19. https://doi.org/10.1016/j.fuel.2018.09.144.

Huang HP, Li J. Molecular composition assessment of biodegradation influence at extreme levels—a case study from oilsand bitumen in the Junggar Basin, NW China. Org Geochem. 2017;103:31–42. https://doi.org/10.1016/j.orggeochem.2016.

Killops SD, Nytoft HP, di Primio R. Biodegradative production and destruction of norhopanes – an example from residual oil in a Paleogene paleomigration conduit on the Utsira High, Norwegian North Sea. Org Geochem. 2019;138:103906. https://doi.org/10.1016/j.orggeochem.2019.103906.

Larter SR, Huang HP, Adams J, et al. A practical biodegradation scale for use in reservoir geochemical studies of biodegraded oils. Org Geochem. 2012;45:66–76. https://doi.org/10.1016/j.orggeochem.2012.01.007.

Larter S, Huang H, Adams J, et al. The controls on the composition of biodegraded oils in the deep subsurface: part II—Geological controls on subsurface biodegradation fluxes and constraints on reservoir-fluid property prediction. AAPG Bull. 2006;90(6):921–38. https://doi.org/10.1306/01270605130.

Li ZX, Huang HP. Bulk and molecular composition variations of gold-tube pyrolysates from severely biodegraded Athabasca bitumen. Pet Sci. 2020. https://doi.org/10.1007/s12182-020-00484-4.

Lin LH, Michael GH, Kovachev G, et al. Biodegradation of tar-sands bitumens from the Ardmore and Anadarko basins, Carter County, Oklahoma. Org Geochem. 1989;14:511–23. https://doi.org/10.1016/0146-6380(89)90031-4.

López L, Mónaco SL, Volkman JK. Evidence for mixed and biodegraded crude oils in the Socororo field, Eastern Venezuela Basin. Org Geochem. 2015;82:12–21. https://doi.org/10.1016/j.orggeochem.2015.02.006.

López L. Study of the Biodegradation levels of oils from the Orinoco Oil Belt (Junin Area) using different biodegradation scales. Org Geochem. 2014;66:60–9. https://doi.org/10.1016/j.orggeochem.2013.

Mao LX, Chang XC, Xu YD, et al. Geochemical characterization and possible hydrocarbon contribution of the Carboniferous interval natively developed in the Chepaizi Uplift of Junggar Basin, northwestern China. Energy Explor Exploit. 2020;38(3):654–81. https://doi.org/10.1177/0144598719892901/.

Marcano N, Larter SR, Mayer B. The impact of severe biodegradation on the molecular and stable (C, H, N, S) isotopic compositions of oils in the Alberta Basin, Canada. Org Geochem. 2013;59:114–32. https://doi.org/10.1016/j.orggeochem.2013.04.001.

Meng FY, Cao Y, Cui Y, et al. Genesis of Carboniferous volcanic reservoirs in Chepaizi salient in western margin of Jungar Basin. J China Univ Pet. 2016;40(5):22–31 **(in Chinese)**.

Miao C, Fu A, Gua L, et al. Reservoir space characteristics and favorable area prediction of volcanic rocks in Chepaizi area, Junggar Basin. Pet Geol Recov Efficien. 2015;33:27–31 **(in Chinese)**.

Moldowan JM, Dahl J, McCaffrey MA, et al. Application of biological marker technology to bioremediation of refinery by-products. Energy Fuels. 1995;9:155–62. https://doi.org/10.1016/0140-6701(95)80752-7.

Ni MJ, Chen S, Liu ZC, et al. Structural evolution of Chepaizi Uplift and its control on stratigraphic deposition in the western Junggar Basin, China. Acta Geol Sin. 2019;93(4):1060–75. https://doi.org/10.1111/1755-6724.13854.

Peters KE, Moldowan JM. The biomarker guide: interpreting molecular fossils in petroleum and ancient sediments. Englewood Cliffs: Prentice Hall; 1993.

Peters KE, Moldowan JM, McCaffrey MA, et al. Selective biodegradation of extended hopanes to 25-norhopanes in petroleum reservoirs,Insight from molecular mechanics. Org Geochem. 1996;24:765–83. https://doi.org/10.1016/s0146-6380(96)00086-1.

Peters KE, Walters CC, Moldowan JM. The Biomarker Guide (Volume 2). London: Cambridge University Press; 2005.

Reed WE. Molecular compositions of weathered petroleum and comparison with its possible source. Geochim Cosmochim Acta. 1977;41:237–47. https://doi.org/10.1016/0016-7037(77)90231-9.

Rullkotter J, Wendisch D. Microbial alteration of 17α(H)-hopane in Madagascar asphalts: removal of C-10 methyl group and ring opening. Geochim Cosmochim Acta. 1982;46:1543–53. https://doi.org/10.1016/0016-7037(82)90313-1.

Seifert WK, Moldowan JM, Demaison GJ. Source correlation of biodegraded oils. Org Geochem. 1984;6:633–43. https://doi.org/10.1016/0146-6380(84)90085-8.

Shi BB, Chang XC, Xu YD, et al. Charging history and fluid evolution for the Carboniferous volcanic reservoirs in the western Chepaizi Uplift of Junggar Basin as determined by fluid inclusions and basin modelling. Geol J. 2020;55:2591–614. https://doi.org/10.1002/gj.3527.

Song C, He L, Ma L, et al. Characteristic of hydrocarbon accumulation of Chepaizi Swell in Junggar Basin. Xinjiang Pet Geol. 2007;28(2):136–8 **(in Chinese)**.

Song MS, Lv MJ, Zhao LQ, et al. Hydrocarbon potential and accumulation model in Chepaizi Uplift, Junggar Basin. China Pet Explor. 2016;21(3):83–91 **(In Chinese)**.

Wang GL, Wang T-G, Simoneit BRT, et al. Investigation of hydrocarbon biodegradation from a downhole profile in Bohai Bay Basin: implications for the origin of 25-norhopanes. Org Geochem. 2013;55:72–84. https://doi.org/10.1016/j.orggeochem.2012.11.009.

Wang HJ, Ma F, Tong XG, et al. Assessment of global unconventional oil and gas resources. Pet Explor Dev. 2016;43(6):925–40. https://doi.org/10.1016/s1876-3804(16)30111-2.

Wardroper AMK, Hoffmann CF, Maxwell JR, et al. Crude oil biodegradation under simulated and natural conditions–2. Aromatic steriod hydrocarbons. Org Geochem. 1984;6:605–17. https://doi.org/10.1016/0146-6380(84)90083-4.

Wenger LM, Davis CL, Isaksen GH. Multiple controls on petroleum biodegradation and impact on oil quality. SPE Reservoir Eval Eng. 2002;5:375–83. https://doi.org/10.2118/80168-pa.

Wenger LM, Isaksen GH. Control of hydrocarbon seepage intensity on level of biodegradation in sea bottom sediments. Org Geochem. 2002;33:1277–92. https://doi.org/10.1016/s0146-6380(02)00116-x.

Williams JA, Bjorøy M, Dolcater DL, et al. Biodegradation in South Texas Eocene oils – effects on aromatics and biomarkers. Org Geochem. 1986;10:451–61. https://doi.org/10.1016/0146-6380(86)90045-8.

Xi W, Zhang Z, Wang X. Oil source analysis and geochemical characteristics of heavy oil in Chunfeng Oilfield. Complex Hydrocarbon Reservoirs. 2014;7(4):19–23 **(in Chinese)**.

Xiao F, Liu L, Zeng L. Geochemical characteristics and oil source of crude oils in the east edge of Chepaizi high, Junggar Basin. J China Univ Min Technol. 2014;43:646–55 **(in Chinese)**.

Xu YD, Chang XC, Shi BB, et al. Geochemistry of severely biodegraded oils in the Carboniferous volcanic reservoir of the Chepaizi Uplift, Junggar Basin, NW China. Energy Explor Exploit. 2018;36(6):1461–81. https://doi.org/10.1177/0144598718770692.

Yin PF, Liu GD, Liu YQ, et al. Evaluation of oil sands resources—a case study in the Athabasca Oil Sands, NE Alberta, Canada. Pet Sci. 2013;10:30–7. https://doi.org/10.1007/s12182-013-0246-9.

Zhang JH, Feng ZH, Fang W, et al. Crude oil hydrocarbon composition characteristics and oil viscosity prediction in the northern Songliao Basin. Sci China Earth Sci. 2014a;57:297–312. https://doi.org/10.1007/s11430-013-4656-8.

Zhang SC, Huang HP, Su J, et al. Geochemistry of Paleozoic marine oils from the Tarim Basin, NW China. Part 4: paleobiodegradation and oil charge mix. Org Geochem. 2014b;67:41–57. https://doi.org/10.1016/j.orggeochem.2013.12.008.

Zhang Z, Xiang K, Qin L, et al. Geochemical characteristics of source rocks and their contribution to petroleum accumulation of Chepaizi area in Sikeshu depression, Junggar Basin. Geol China. 2012;39:326–37 **(in Chinese)**.

Zhao WZ, Hu SY, Guo XJ, et al. New concepts for deepening hydrocarbon exploration and their application effects in the Junggar Basin, NW China. Pet Explor Dev. 2019;46(5):856–65. https://doi.org/10.1016/S1876-3804(19)60245-4.

Zhou SQ, Huang HP, Liu YM. Biodegradation and origin of oil sands in the Western Canada Sedimentary Basin. Pet Sci. 2008;15(2):87–94. https://doi.org/10.1007/s12182-008-0015-3.